Proceedings of DETC'03
ASME 2003 Design Engineering Technical Conferences and
Computers and Information in Engineering Conference
Chicago, Illinois, USA, September 2-6, 2003

DETC2003/VIB-48480

MODELING AND NUMERICAL INVESTIGATION OF NON-LINEAR DYNAMICS OF A MONO-CYLINDER COMBUSTION ENGINE

Jan Awrejcewicz and Grzegorz Kudra
Technical University of Lodz
Department of Automatics and Biomechanics
1/15 Stefanowskiego St., 90-924 Lodz, Poland
E-mail: awrejcew@p.lodz.pl and grekudra@p.lodz.pl

ABSTRACT

A mono-cylinder combustion engine is modeled as the triple physical pendulum with barriers. The proposed model exhibits well known six stages of sliding of a piston along a cylinder per engine cycle and it can be useful while investigating impacts between the piston and the cylinder.

1 INTRODUCTION

Many real processes like earth-quake caused vibrations of high buildings can be modeled via coupled pendulums. It is clear that a couple system of pendulums may exhibit more complex nonlinear dynamics than a single harmonically or parametrically excited pendulum (see references (Awrejcewicz et al., 2002; Bishop and Clifford, 1996; Szemplińska-Stupnicka and Tyrkiel, 2002a, 2002b; Szemplińska-Stupnicka et al., 2000)). In addition, one may expect that many theoretical unsolved problems of nonlinear dynamics can be explained using a model of rigid multi-body coupled pendulums.

Our research is mainly focused on application of triple pendulum dynamics to a real world object. In spite of neglecting of many technological and design-oriented details, an inverted triple pendulum can be used to model a real piston – connecting rod – crankshaft system of a mono-cylinder combustion engine.

Problems of modeling of multi-body systems with activity state of constraints varying during dynamics are addressed in references (Ballard, 2000; Pfeiffer, 1999; Wösle and Pfeiffer, 1999). On the other hand, the problem of stiff impacts in multi-body systems is illustrated and discussed in the monograph (Brogliato, 1999).

2 PISTON – CONNECTING ROD – CRANKSHAFT SYSTEM

The general model of the triple physical pendulum with barriers (Awrejcewicz et al., 2001, 2002; Kudra, 2002) can be used to build a model of the piston – connecting rod – crankshaft system of the mono-cylinder combustion engine shown in Figure 1. The first link represents the crankshaft (1), the second one is the connecting rod (2) and the third one is the piston (3). It is assumed that the links are absolute stiff bodies moving in a vacuum, in the plane of a global co-ordinate system $\bar{x}, \bar{y}$ (with origin in the point O_1). The links are connected in points O_i (i=1,2,3) by rotational joints with viscous damping of real coefficients $\bar{c}_i$ correspondingly. The points c_i are the mass centers of the corresponding bodies and the position of the system is described by three angles φ_i (i=1,2,3).

The cylinder barrel imposes restrictions on the piston position, which moves in the cylinder with backlash. It is assumed that in the contact of the surfaces between the piston and the cylinder, a tangent force does not appear.

It is assumed that a gas pressure force $\bar{F}(\varphi_1)$ is a function of the angular position of the crankshaft φ_1 and can be reduced to the force acting along line parallel to the axis of the cylinder and containing the piston pin axis O_3. Moreover, the crankshaft is externally driven by the moment $\bar{M}_0$ originating from an external power receiver (brake) and acting contrary to the positive sense of the angle φ_1. We assume also that the rotational speed of the crankshaft is positive.

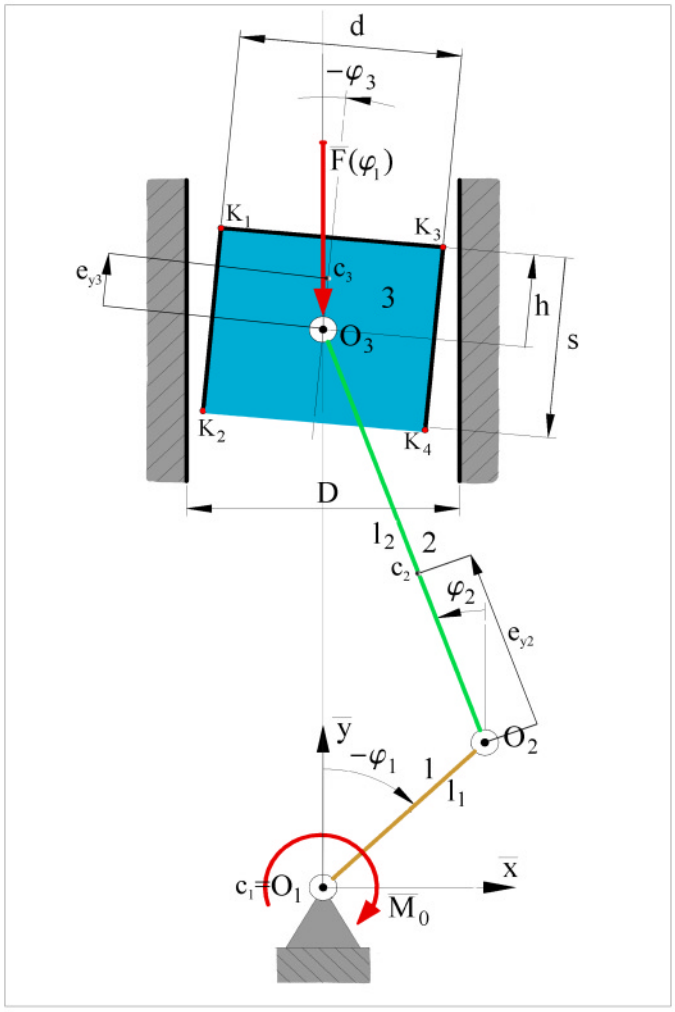

Fig. 1 Piston – connecting rod – crankshaft system.

The non-dimensional equations of motion, when non of the obstacles is active, are as follows

$$\mathbf{M}(\boldsymbol{\varphi})\ddot{\boldsymbol{\varphi}}+\mathbf{N}(\boldsymbol{\varphi})\dot{\boldsymbol{\varphi}}^{\mathbf{2}}+\boldsymbol{\epsilon}\dot{\boldsymbol{\varphi}}=\mathbf{f}_e(\boldsymbol{\varphi}), \tag{1}$$

where

$$\boldsymbol{\varphi}=\begin{Bmatrix}\varphi_1\\ \varphi_2\\ \varphi_3\end{Bmatrix},\quad \ddot{\boldsymbol{\varphi}}=\begin{Bmatrix}\ddot{\varphi}_1\\ \ddot{\varphi}_2\\ \ddot{\varphi}_3\end{Bmatrix},\quad \dot{\boldsymbol{\varphi}}^{\mathbf{2}}=\begin{Bmatrix}\dot{\varphi}_1^2\\ \dot{\varphi}_2^2\\ \dot{\varphi}_3^2\end{Bmatrix},\quad \dot{\boldsymbol{\varphi}}=\begin{Bmatrix}\dot{\varphi}_1\\ \dot{\varphi}_2\\ \dot{\varphi}_3\end{Bmatrix}, \tag{2a}$$

$$\mathbf{M}(\boldsymbol{\varphi})=\begin{bmatrix}1 & \nu_{12}\cos(\varphi_1-\varphi_2) & \nu_{13}\cos(\varphi_1-\varphi_3)\\ \nu_{12}\cos(\varphi_1-\varphi_2) & \beta_2 & \nu_{23}\cos(\varphi_2-\varphi_3)\\ \nu_{13}\cos(\varphi_1-\varphi_3) & \nu_{23}\cos(\varphi_2-\varphi_3) & \beta_3\end{bmatrix}, \tag{2b}$$

$$\mathbf{N}(\boldsymbol{\varphi})=\begin{bmatrix}0 & \nu_{12}\sin(\varphi_1-\varphi_2) & \nu_{13}\sin(\varphi_1-\varphi_3)\\ -\nu_{12}\sin(\varphi_1-\varphi_2) & 0 & \nu_{23}\sin(\varphi_2-\varphi_3)\\ -\nu_{13}\sin(\varphi_1-\varphi_3) & -\nu_{23}\sin(\varphi_2-\varphi_3) & 0\end{bmatrix}, \tag{2c}$$

$$\boldsymbol{\epsilon}=\alpha_1^{-1}c_1\begin{bmatrix}1+c_{21} & -c_{21} & 0\\ -c_{21} & c_{21}+c_{31} & -c_{31}\\ 0 & -c_{31} & c_{31}\end{bmatrix}, \tag{2d}$$

$$\mathbf{f}_e(\boldsymbol{\varphi})=\alpha_1^{-2}\begin{Bmatrix}F_0\,p(\varphi_1)\sin\varphi_1-M_0\\ \lambda_2 F_0\,p(\varphi_1)\sin\varphi_2\\ 0\end{Bmatrix}, \tag{2e}$$

where the symbols $(\overset{\circ}{...})$ and $(\overset{\circ\circ}{...})$ denote respectively the first and second derivatives with respect to the non-dimensional time t, and the following non-dimensional parameters are used

$$\beta_2=\frac{B_2}{B_1},\ \beta_3=\frac{B_3}{B_1},$$
$$\nu_{12}=\frac{N_{12}}{B_1},\ \nu_{13}=\frac{N_{13}}{B_1},\ \nu_{23}=\frac{N_{23}}{B_1}, \tag{3a}$$

$$\alpha_1=\alpha_1^{-1}\frac{\pi n}{30}, \tag{3b}$$

$$c_1=\frac{F_0(1-\eta_m)\int_0^{2\pi N}p(\varphi_1)\sin\varphi_1\left(1+\dfrac{\cos\varphi_1}{\lambda_2\sqrt{1-\lambda_2^{-2}\sin^2\varphi_1}}\right)d\varphi_1}{2\pi N\left((1+c_{21})+\lambda_2^{-1}(c_{21}+c_{31})\left(1-\sqrt{1-\lambda_2^{-2}}\right)\right)\alpha_1}, \tag{3c}$$

$$c_{21}=\frac{\bar{c}_2}{\bar{c}_1},\ c_{31}=\frac{\bar{c}_3}{\bar{c}_1}, \tag{3d}$$

$$M_0=\frac{\eta_m F_0\int_0^{2\pi N}p(\varphi_1)\sin\varphi_1\left(1+\dfrac{\cos\varphi_1}{\lambda_2\sqrt{1-\lambda_2^{-2}\sin^2\varphi_1}}\right)d\varphi_1}{2\pi N}, \tag{3e}$$

$$F_0=p_{\max}\frac{\pi d^2}{4}\frac{l_1}{M_1}, \tag{3f}$$

$$\lambda_2=\frac{l_2}{l_1}, \tag{3g}$$

where n [rot./min.] represents the real average rotational speed of the crankshaft, p_{max} is the maximal pressure over the piston, and $p(\varphi_1)$ is the non-dimensional pressure distribution with period $2\pi N$ (where N is an integer number) such that its maximal value is one and η_m is the mechanical efficiency of the engine, i.e. $\eta_m=-L_M/L_F$, where L_M is the $\bar{M}_0$ force work

and L_F is the $\overline{F}(\varphi_1)$ force work. In the expressions (3) the following notation is used

$$\begin{aligned} B_1 &= J_{z1} + l_1^{\,2}(m_2 + m_3), \\ B_2 &= J_{z2} + e_{y2}^{\,2} m_2 + l_2^{\,2} m_3, \\ B_3 &= J_{z3} + e_{y3}^{\,2} m_3, \end{aligned} \tag{4a}$$

$$\begin{aligned} N_{12} &= m_2 e_{y2} l_1 + m_3 l_1 l_2, \\ N_{13} &= m_3 e_{y3} l_1, \\ N_{23} &= m_3 e_{y3} l_2, \end{aligned} \tag{4b}$$

$$M_1 = (m_2 + m_3) g\, l_1, \tag{4c}$$

$$\alpha_1 = \left(M_1 B_1^{-1}\right)^{\frac{1}{2}}. \tag{4d}$$

In the above J_{zi} (i=1,2,3) denote moments of inertia of the appropriate links with respect to the principal central axes perpendicular to the movement plane, whereas m_i (i=1,2,3) denote masses of respective links and g is the gravitational acceleration.

Moreover the following relation between non-dimensional time t and the real one τ holds

$$t = \alpha_1 \alpha_1 \tau. \tag{5}$$

Note that some non-dimensional parameters refer to the dimensional ones by the use of terms with the gravitational acceleration g, but in the final form of the governing equations (1) the gravitational forces are neglected (Awrejcewicz et al., 2001, 2002; Kudra, 2002). The presented here model of the piston-connecting rod-crank shaft system serves as a special case of the earlier triple physical pendulum model, in which the non-dimensional time is scaled in such a way that the non-dimensional angular velocity of the shaft is approximately equal to one. Moreover, more convenient setting of the system parameters in the case of the engine model is introduced, i.e. a user of the program should give the gas pressure parameters, the mechanical efficiency of the system and the ratios of appropriate damping coefficients. Both external power receiver moment and absolute damping coefficients do not require a definition.

A restriction on the piston position imposed by the cylinder barrel can be described using the following non-dimensional set of inequalities (representing stiff unilateral constraints):

$$\begin{aligned} h_1(\boldsymbol{\varphi}) &= \frac{\Delta}{2} - \sin\varphi_1 - \lambda_2 \sin\varphi_2 - \eta \sin\varphi_3 - \frac{\delta}{2}\cos\varphi_3 \geq 0, \\ h_2(\boldsymbol{\varphi}) &= \frac{\Delta}{2} - \sin\varphi_1 - \lambda_2 \sin\varphi_2 + (\sigma - \eta)\sin\varphi_3 - \frac{\delta}{2}\cos\varphi_3 \geq 0, \\ h_3(\boldsymbol{\varphi}) &= \frac{\Delta}{2} + \sin\varphi_1 + \lambda_2 \sin\varphi_2 + \eta \sin\varphi_3 - \frac{\delta}{2}\cos\varphi_3 \geq 0, \\ h_4(\boldsymbol{\varphi}) &= \frac{\Delta}{2} + \sin\varphi_1 + \lambda_2 \sin\varphi_2 - (\sigma - \eta)\sin\varphi_3 - \frac{\delta}{2}\cos\varphi_3 \geq 0, \end{aligned} \tag{6}$$

where

$$\eta = \frac{h}{l_1},\ \sigma = \frac{s}{l_1},\ \delta = \frac{d}{l_1},\ \Delta = \frac{D}{l_1}, \tag{7}$$

and the same restitution coefficient e is related to each of the unilateral constraints.

Observe that the proposed dynamical model of the piston – connecting rod – crankshaft system can be treated as a simplified model, since some very important technological details are neglected. The most important simplifications follow: (i) tangent forces of interaction between the surfaces of the piston and the cylinder are neglected; (ii) interaction of the piston-cylinder introduced by the piston rings (by means of friction forces in the ring grooves in direction perpendicular to the cylinder surface) is neglected; (iii) simplified friction model in every joint of the system (i.e. linear damping) is assumed.

In addition, modelling of an impact between the piston and the cylinder, where an oil layer exists, requires an approach different from the generalized restitution coefficient rule.

In other words, a detailed modelling of the piston – connecting rod – crankshaft system with all essential technological details exceeds scope of this work. However, we believe that the general model of the triple physical pendulum presented in section 2 and being the subject of some earlier works (Awrejcewicz et al., 2001, 2002; Kudra, 2002) can serve as a good starting point for the more advanced and close to reality dynamical model of the piston – connecting rod – crankshaft system, taking into account lateral motion and impacts between the piston and the cylinder barrel.

It should be also noticed that the presented model can govern steady state solutions of the system, and the simulated transient motion does not correspond to the real piston – connecting rod – crankshaft system.

Dynamics of the piston – connecting rod – crankshaft system has been rigorously studied in the Habilitation Thesis (Sygniewicz, 1991). Although the model presented by Sygniewicz satisfies the assumed role, it does not take into account the full piston dynamics including a lateral motion of the piston in the cylinder barrel. In contrary, our proposed full dynamical model of the piston – connecting rod – crankshaft system governs in full dynamics of the piston analysis including impacts between the piston and the cylinder.

The full employed computational model is not presented here (see for details (Awrejcewicz and Kudra, 2003; Kudra, 2002)). In particular, the integral part of the system state (besides the generalized co-ordinate and velocities vectors) is the state of each potentially active constraints, described by the appropriate index sets (Ballard, 2000; Pfeiffer, 1999; Wösle

and Pfeiffer, 1999). Each of the constraints can be inactive, in the state of impact or in the state of sliding.

The impact is modelled by the use of generalized Newton's impact law concept, based on the restitution coefficient (Brogliato, 1999). A sliding state is defined by a continuous contact between the system body and the surface of the barrier. It is modelled by the use of Lagrangian multipliers, which represent normal reactions from the barrier surface acting on the system.

The Runge-Kutta integration within the time intervals between each two successive discontinuity points is applied. The discontinuity points are the points of change of the activity state of any constraints (i.e. impact event, or the beginning or end of the sliding state), and they are detected by halving the time step until the assumed precision is obtained.

3 NUMERICAL EXAMPLES

In this section the non-dimensional pressure distribution function $p(\varphi_1)$ shown in Figure 2 is used applying the data included in reference work (Sygniewicz, 1991), and concerning the real pressure function obtained experimentally from the engine 1HC102. The period of the function is 4π (N=2 for the four-stroke engine), maximal pressure p_{max}=8MPa for the rotational crankshaft speed n=1200 [rot./min.] and the full engine loading.

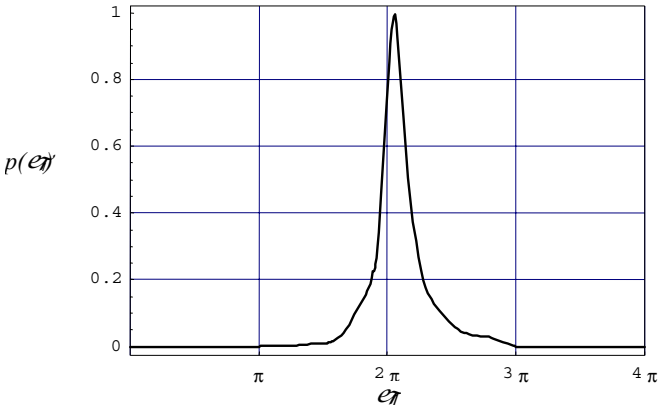

Fig. 2 Gas pressure function used for calculations.

The function $p(\varphi_1)$ is developed into the Fourier series with K=25 terms. The rest of parameters are as follows: $m_1 = 10$ kg, $m_2 = 1$ kg, $m_3 = 0.4$ kg, $J_{z1} = 1$ kg m^2, $J_{z2} = 0.0075$ kg m^2, $J_{z3} = 0.001$ kg m^2, $l_1 = 0.04$ m, $l_2 = 0.15$ m, $e_{y1} = 0$ m, $e_{y2} = 0.12$ m, $e_{y3} = 0.01$ m, $d = 0.08$ m, $s = 0.08$ m, $h = 0.04$ m, $\eta_m = 0.85$, $c_{21} = 0.2$, $c_{31} = 0.1$, $g = 9.81$ ms^{-2}. The following real parameters are found owing to the introduced values: $\overline{M}_0 = 24.7$ Nm and $\overline{c}_1 = 0.0288$ Nm^{-1}s. The calculations are performed for different values of the restitution coefficient and the external diameter D.

The zero initial conditions in the time instant $t = 0$ are applied in all further shown examples. In Figures 3-8 the steady state solution is shown within the time interval $t \in (5000,5500)$.

The following non-dimensional co-ordinates describing a position of the piston pin axis are used

$$x_{O3} = \frac{\overline{x}_{O3}}{l_1} = -\sin\varphi_1 - \lambda_2 \sin\varphi_2 ,$$
$$y_{O3} = \frac{\overline{y}_{O3}}{l_1} = \cos\varphi_1 + \lambda_2 \cos\varphi_2 . \qquad (8)$$

The response of the system for the restitution coefficient e=0 and the cylinder diameter D=0.08008 m. (the backlash of the piston in the barrel is 0.08 mm) is shown in Figure 3. It is seen from the figures that the piston six times moves from one side of the cylinder to the second side during one cycle of the engine work, and most of the time the piston adjoins either to one or second side of the cylinder surface. This result confirms the investigations presented in the work (Sygniewicz, 1991). However, the piston loses contact with cylinder moving from one side to the second side of the cylinder with a small rotation angle. This phenomenon differs from results presented in reference (Sygniewicz, 1991). Namely, it was assumed that the piston do not loose the contact with cylinder. The crankshaft angular positions in beginnings and ends of the phases of the piston adjoining and sliding along the cylinder (see the example shown in Fig. 3) differ also from results presented by (Sygniewicz, 1991) up to 35°. In the latter case, the exhibited differences follow from neglected by us some essential technological details mentioned in the previous section.

In Figure 4, the results for the larger restitution coefficient , i.e. e=0.5 are shown. It is seen that the states of the piston adjoining to the cylinder surface are in general the same as previously. Only the beginning of each of them is slightly delayed, since the piston bounces against the cylinder few times before sliding occurs. Figure 5 contains successive piston positions yielded by this solution. The results for the restitution coefficient e=0.9 (Figure 6) for five times larger backlash between the cylinder and the piston (D=0.08040 m), and for the restitution coefficients e=0.5 (Figure 7) and e=0.9 (Figure 8) are also reported. It is worth noticing that the system has at least inclination to reach the same states of the piston adjoining and sliding along the cylinder, and lasting in the same crankshaft positions as previously. Since multiple impacts between piston and cylinder occur, it happens that the piston rapidly leaves the contact and transits into a second cylinder side.

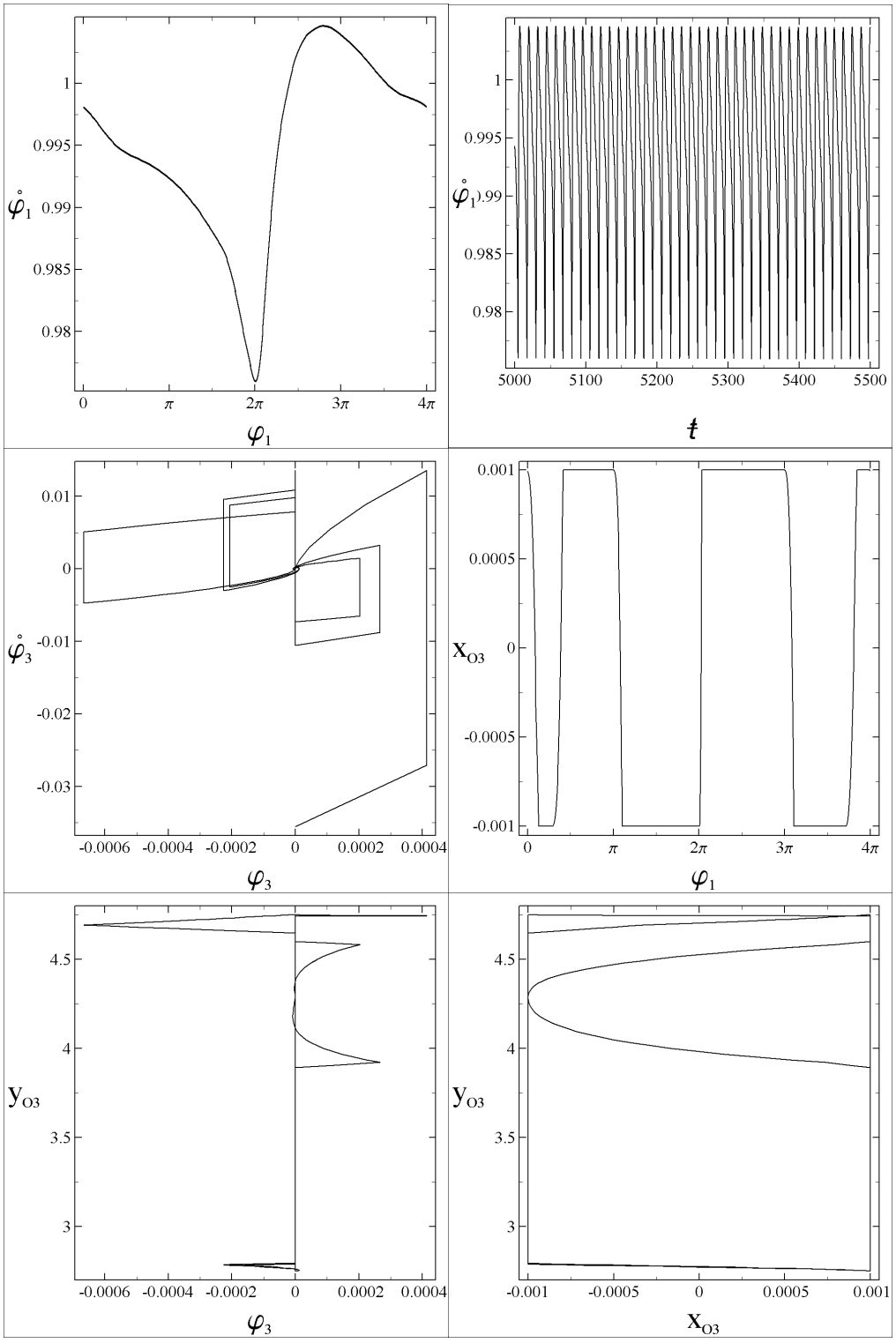

Fig. 3 Response of the system for *e*=0 and *D*=0.08008 m.

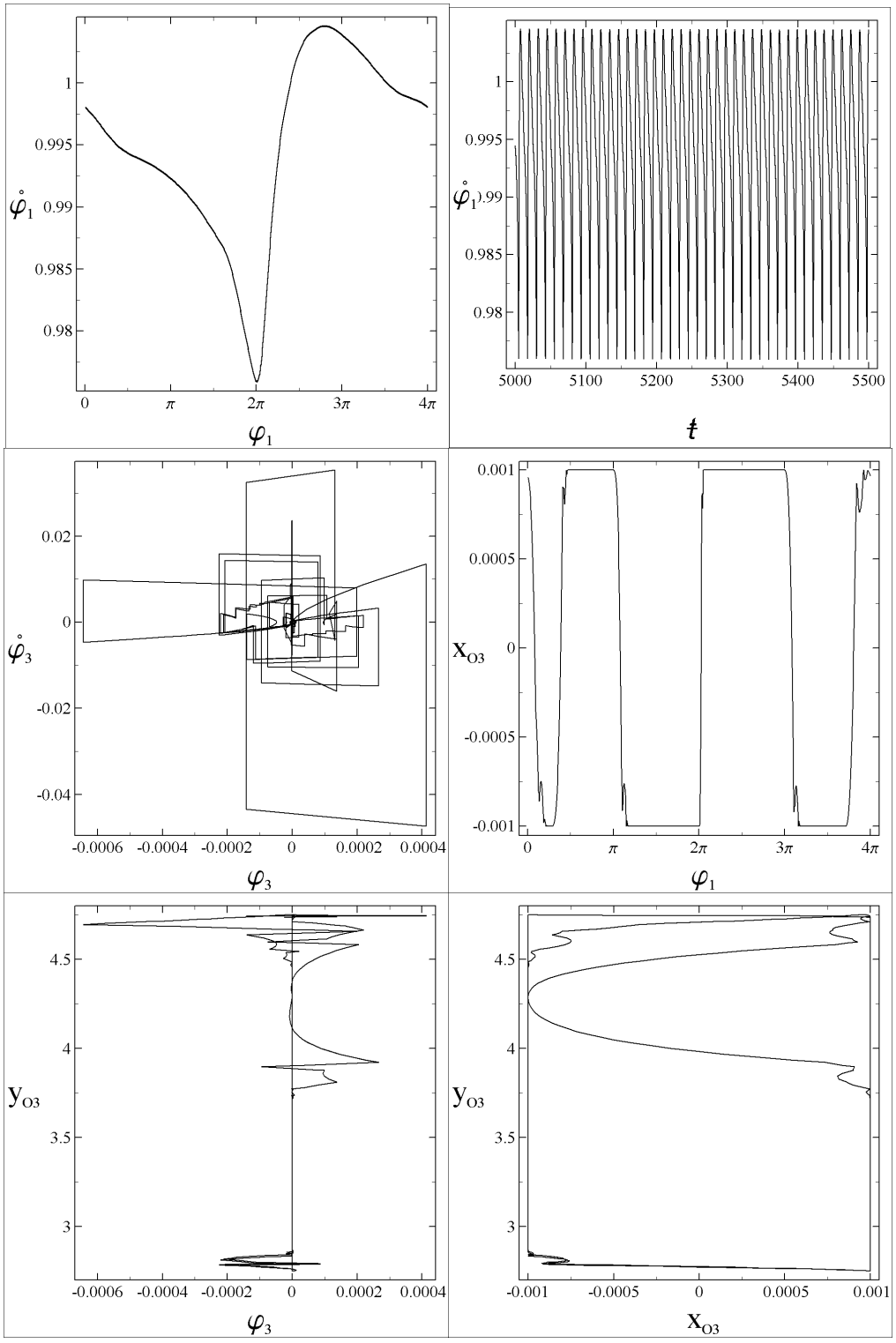

Fig. 4 Response of the system for *e*=0.5 and *D*=0.08008 m.

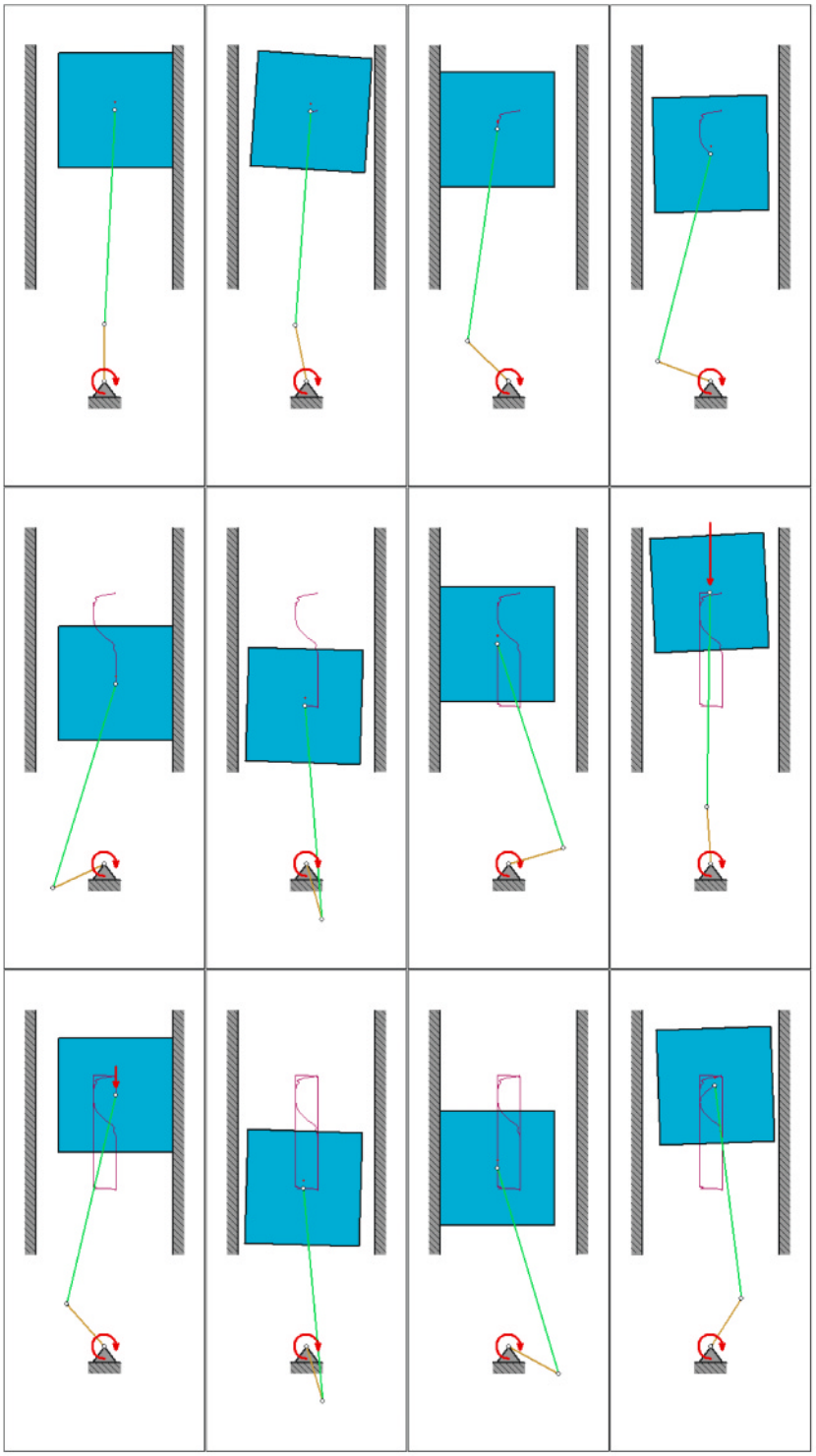

Fig. 5 The successive positions composition of the piston in cylinder barrel for *e*=0.5 and *D*=0.08008 m.

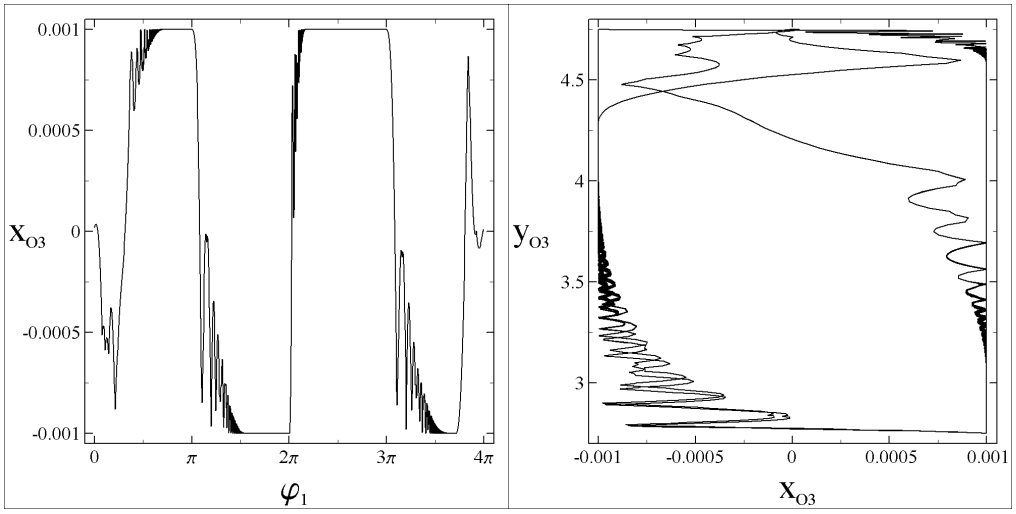

Fig. 6 Response of the system for *e*=0.9 and *D*=0.08008 m.

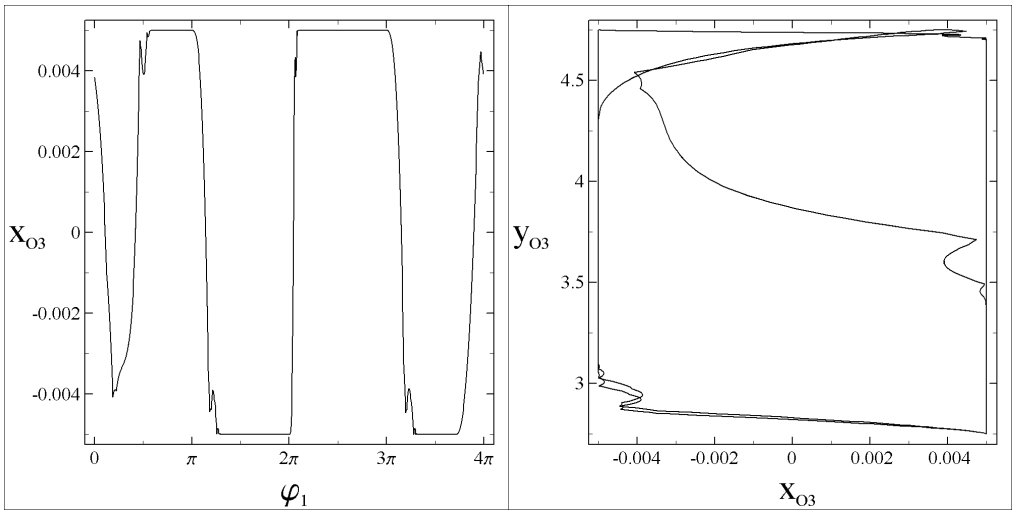

Fig. 7 Response of the system for *e*=0.5 and *D*=0.08040 m.

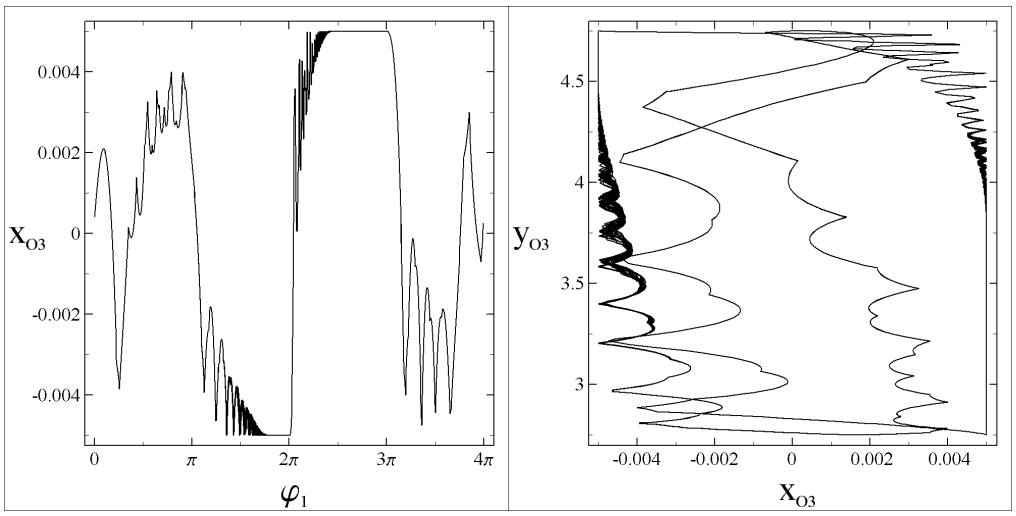

Fig. 8 Response of the system for *e*=0.9 and *D*=0.0840 m.

4 CONCLUDING REMARKS

A piston – connecting rod – crankshaft modeled as the triple physical pendulum with impacts (in spite of some differences) behaves in a way similar to that described and illustrated in the monograph (Sygniewicz, 1991). In particular, six piston movements from one side of the cylinder to its opposite side (during one cycle of the engine work) have been detected. Mainly lasting states of the piston adjoining and sliding along one or the second side of the cylinder surface have been observed. The presented model can be treated as the first step to describe the real piston-connecting rod-crankshaft system, and after taking account of some technological details the better convergence with real system behavior can be expected. Moreover, the proposed model describes full dynamics of a piston motion in a cylinder, and hence it can be very useful for the noise analysis generated by impacts between piston and cylinder barrel.

ACKNOWLEDGMENTS

The investigations included in this work have been supported by the Polish Scientific Research Committee (KBN) under the grant No. 8 T07A 009 21.

REFERENCES

Awrejcewicz, J., Kudra, G. and Lamarque C.-H. “Analysis of bifurcations and chaos in three coupled physical pendulums with impacts,” *Proceedings of Design Engineering Technical Conferences,* Pittsburgh, CD-ROM, 8 pages, 2001.

Awrejcewicz, J., Kudra, G. and Lamarque C.-H. “Dynamics investigation of three coupled rods with a horizontal barrier,” *Meccanica* (to appear), 2003.

Awrejcewicz, J., Kudra, G. and Lamarque C.-H. “Nonlinear dynamics of triple pendulum with impacts,” *Journal of Technical Physics,* 43, 97-112, 2002.

Awrejcewicz, and J., Kudra, G. “The piston – connecting rod – crankshaft system as a triple physical pendulum with impacts,” *Int. J. Bifurcation and Chaos* (to appear), 2003.

Ballard, P. “The dynamics of discrete mechanical systems with perfect unilateral constraints,” *Arch. Rational Mech. Anal.*, 154, 199-274, 2000.

Bishop, S. R. and Clifford M. J. “Zones of chaotic behaviour in the parametrically excited pendulum,” *J. Sound Vib.* **189**(1), 142-147, 1996.

Brogliato, B. *Nonsmooth Mechanics* (Springer-Verlag, London) Chap. 6, 263-282, 1999.

Kudra, G. “Analysis of bifurcation and chaos in the triple physical pendulum with impacts,” PhD thesis, Technical University of Łódź, in Polish, 2002.

Pfeiffer, F. “Unilateral problems of dynamics,” *Archive of Applied Mechanics,* 69, 503-527, 1999.

Sygniewicz, J. *Modeling of cooperation of the piston with piston rings and barrel*, Scientific Bulletin of Łódź Technical University **615/149**, in Polish, 1999.

Szemplińska-Stupnicka, W. and Tyrkiel, E. "Common features of the onset of structurally stable chaos in nonlinear oscillators: A phenomenological approach," *Nonlin. Dyn.* **27**, 1-25, 2002.

Szemplińska-Stupnicka, W. and Tyrkiel, E. “The oscillation-rotation attractors in a forced pendulum and their peculiar properties,” *Int. J. Bifurcation and Chaos* **12**(1), 159-168, 2002.

Szemplińska-Stupnicka, W., Tyrkiel, E. and Zubrzycki, A. “The global bifurcations that lead to transient tumbling chaos in a parametrically driven pendulum,” *Int. J. Bifurcation and Chaos* **10**(9), 2161-2175, 2000.

Wösle, M. and Pfeiffer, F. “Dynamics of spatial structure-varying rigid multibody systems,” *Archive of Applied Mechanics*, 69, 265-285, 1999.